fib WILEY

Structural behavior of multifunctional inhomogeneous infra-lightweight concrete elements

Claudia Lösch ⬤ | Arno Richter | Mike Schlaich

Chair of Conceptual and Structural Design, Technische Universität Berlin, Berlin, Germany

Correspondence
Claudia Lösch, Technische Universität Berlin, Fachgebiet Entwerfen und Konstruieren - Massivbau, TIB1-B2, Claudia Lösch, Gustav-Meyer-Allee 25, 13355 Berlin, Germany.
Email: claudia.loesch@tu-berlin.de

Abstract

The reduction of energy and resources consumption in the building sector is of crucial importance. One way to approach this challenge is the development of high-performance materials to increase efficiency. In the research project "MultiLC" (Multifunctional lightweight concrete elements with inhomogeneous properties) highly efficient Infra-Lightweight Concrete (ILC) elements with varying properties over the cross-section and further functions, for example, active thermal insulation or photocatalytic air purification, were developed. Besides investigations in concrete technology and building physics, the structural behavior of inhomogeneous ILC-elements was examined. This paper summarizes the analytical and experimental methods used to investigate the structural behavior of wall and beam specimens and wall-to-slab connections. It was found that the stiffness method is a reasonable approach to calculate the maximum load-bearing capacity of the inhomogeneous ILC elements. Recommendations could be formulated for ultimate design values. Also, the feasibility of a fixed connection between a normal concrete slab and a multi-layered ILC-wall was shown.

KEYWORDS

active thermal insulation, functionally graded materials, high performance lightweight aggregate concrete, infra-lightweight concrete, inhomogeneous concrete elements, multifunctional, structural behavior, structural design, wall-to-slab connection

1 | INTRODUCTION

1.1 | Motivation and project outline

The motivation of the 3-year research project MultiLC ("Multifunctional Lightweight Concrete Elements with Inhomogeneous Properties"), funded by the German Federal Ministry of Education and Research (BMBF 13XP5010B), was to add a scientific contribution towards a sustainable construction technique by developing a highly efficient component for the building skin. Starting point was Infra-Lightweight Concrete (ILC), a high-performance lightweight aggregate concrete (HPLWAC) with a dry density below 800 kg/m^3. ILC combines both load-bearing and insulating properties in one single material.[1] Therefore, an ILC exterior, monolithic wall is already a quite efficient high-performance element for

large buildings and eliminates the need for composite insulation systems. One of the aims of the project was to increase efficiency even further by varying the properties of the concrete such as density and strength over the cross section according to the different physical and structural requirements within the section. Hence, areas with higher strength focusing on load-bearing and areas with lower density focusing on heat insulation were created.

In addition, the goal of the MultiLC project was to include further functions such as active thermal insulation techniques and photocatalytic layers for reduction of air pollutants (Figure 1). To achieve this, an interdisciplinary team of material technologists, structural engineers, and building physicists from research institutions and industry (HeidelbergCement, Sika Germany, Transsolar KlimaEngineering, schlaich, bergermann partner and the TU Berlin) operated in several work groups. Subjects of investigation were the control of the fresh and hardened concrete properties, the load-bearing and deformation behavior, as well as simulations of the active thermal insulation and analyses on the life cycle assessment, but also aspects of construction and marketability, such as structural detailing, production processes and costs.

Infra-Lightweight Concrete has been investigated at the Chair of Conceptual and Structural Design, Technische Universität Berlin (TU Berlin), for more than 10 years.[2,3] It stands out from insulating concretes due to an exceptional combination of low density, hence good insulation properties, and comparatively good compressive strength. An example for a recently finished ILC project is the single-storey youth recreation centre in Berlin (Figure 2).
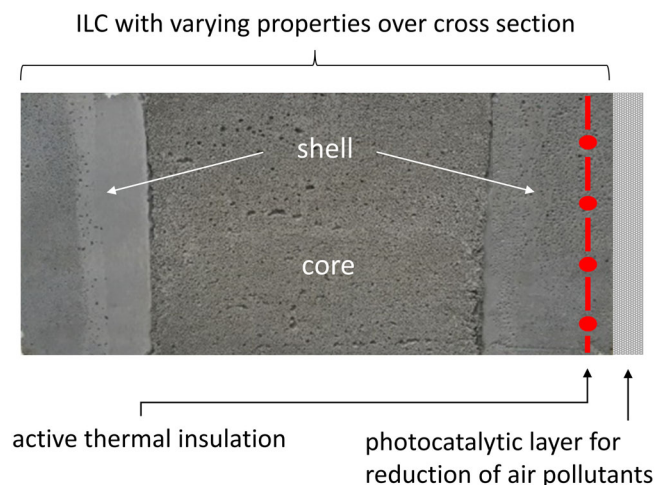

ILC with varying properties over cross section

FIGURE 1 Concept of a multifunctional lightweight concrete element with inhomogeneous properties[8]

The concept of inhomogeneous materials where properties follow function, also called functionally graded materials, is no news. Examples can be found in nature, such as the structure of bones or bamboo. The term "Functionally Graded Materials" was mainly implemented in material research and has been used since the 1970s. From 1995 to 2003, a priority program "Functionally Graded Materials" funded by the Deutsche Forschungsgemeinschaft (DFG) was carried out that investigated the concept for metals, ceramics, and polymers.[4] The principle was first applied to concrete at the Stuttgart University in 2006,[5] where functionally graded concrete has been continuously developed since.[6]

The application of inhomogeneous concrete elements in the building skin is also pursued by other research projects. For example, in the h-house project[7] façade elements with functional surfaces, made of UHPC shells and inner autoclaved aerated concrete or cellular lightweight concrete were developed. However, while these components were designed to be non-loadbearing, a major requirement for MultiLC elements is to provide the load-bearing function as well.

This paper summarizes the analytical and experimental methods used to investigate the structural behavior of MultiLC elements and the main findings. The following sections present the investigations regarding inhomogeneous beams, inhomogeneous wall elements and subsequently fixed wall-to-slab connections.

1.2 | Structural behavior of inhomogeneous concrete elements

To describe the structural behavior of inhomogeneous concrete elements, several approaches can be utilized depending on factors such as the structure characteristics, the concrete properties and the complexity of inhomogeneity or grading. Neumann[9] and Trätner[10] describe several methods such as a method based on reference areas, the stiffness method, the finite-element method (FEM), the method of even cross sections and the n_L-method (using the ratio nL of young's modulus of outer and inner layers to determine equivalent cross sectional values of the layers).[9,10] These approaches were used to determine the load bearing capacity of exterior wall elements consisting of a lightweight concrete core with high porosity and outer concrete layers of higher density and higher strength.

With respect to MultiLC-elements, the goal was to find a feasible approach to define structural behavior. Of the methods mentioned above, FEM can theoretically provide the most accurate results and will often be the best approach for structures with highly complex

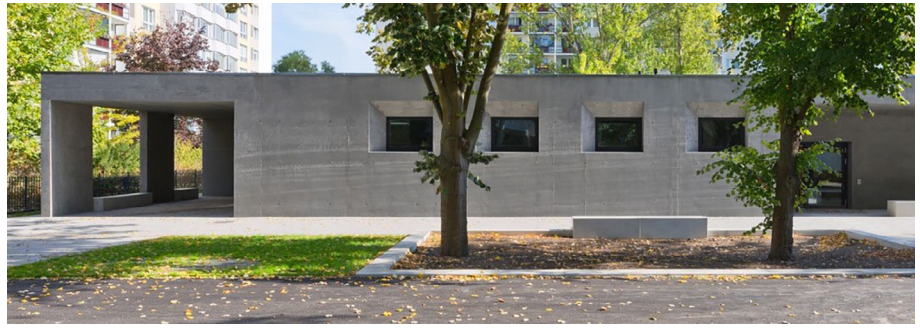FIGURE 2   ILC youth recreation centre in Berlin (Picture: Alexander Blumhoff)

TABLE 1   Exemplary ILC mixes for shell and core concrete (based on[14])

Materials	Units	Shell (ILC 800)	Core (ILC500)
CEM III/A 42.5 N	(kg/m^3)	460	210
$(w/c)_{eq}$		0.40	0.65
Silica fume		100	45
Stabilizer		0.69	0.40
Superplasticizer		3.91	1.47
Expanded glass 0.5/1	(kg/m^3)	85.3	52.9
Expanded glass 1/2		58.5	59.7
Expanded glass 2/4		–	95.9
Expanded clay 2/8		120.2	–
Properties			
Dry density	(kg/m^3)	804	456
Compressive strength	(MPa)	15.8	5.3
Thermal conductivity	(W/mK)	0.169	0.088

inhomogeneity or geometry. FEM has already been successfully applied for inhomogeneous concrete elements in various cases (e.g., [6,11,12]). However, input parameters such as in-depth material properties are crucial for the quality of results and can be very difficult to derive. Therefore, for inhomogeneous concrete elements of little complexity, Neumann[9] concluded that FEM should rather serve for a qualitative assessment of structural behavior, whereas other methods are more feasible for quantitative results.

For MultiLC-elements, the complexity of inhomogeneity was deliberately kept at a low level to keep production processes practicable. After consideration of different cross-section variations, a combination of outer areas with higher strength (shell) and an inner, highly porous area (core) with better heat-insulating properties was chosen[13] (Figure 1). For shell and core, different Infra-Lightweight Concrete mixes based on CEM III A, several lightweight aggregates fractions, silica fume, and several admixtures were developed during the project. Table 1 shows exemplary mixes including main material properties. Elements with such a setup can be casted best in a horizontal position, pouring the concrete for the outer shell layer first, then adding the middle (core) layer, last the inner shell layer. Before pouring the middle and inner layer, some time (several hours depending on environmental conditions) should be allowed for first stiffening of the lower layer to prevent intermixing of the different concrete types.

Generally, the different types of ILC applied in the wall or beam section all show a linear elastic material behavior. Therefore, the configurations of the stress–strain relations are similar, just the gradient, hence the E-Modulus, and the maximum strain levels are different. It is also presumed that plane sections before bending remain plane after bending (Euler–Bernoulli-hypothesis), hence different concrete layers are subjected to the same deformation or strain at interfaces and thus an equal strain distribution over the inhomogeneous cross section is present. Based on these assumptions, the stiffness method was chosen to determine the maximum load bearing capacity of the MultiLC-elements as it is easily manageable and gives good quality results under the mentioned conditions.

The idea of the stiffness method is that loads are attributed to different material layers according to their

stiffness. Depending on the type of loading, either bending stiffness $E \cdot I$ or axial stiffness $E \cdot A$ has to be considered. The calculation is performed for each layer separately and is formulated by Neumann[9] as stated below:

$$\sigma_i = \left(\frac{N}{A_{ges}} \cdot \frac{E_i \cdot A_i}{\sum\limits_{i=1}^{n} E_i \cdot A_i} + \frac{M}{W_{ges}} \cdot \frac{E_i \cdot I_i}{\sum\limits_{i=1}^{n} E_i \cdot I_i} \right) \cdot \frac{A_{ges}}{A_i} \quad (1)$$

$$\leq \frac{\beta_{R,i}}{\gamma_i} \, [\text{N/mm}^2]$$

where σ_i is the stress of considered layer (N/mm^2); i is the number of considered layer; N is the axial load (N); A_{ges} is the total area (mm^2); E_i is the Young's modulus of considered layer (N/mm^2); A_i is the area of considered layer (mm^2); n is the total number of layers; M is the bending moment (Nmm); W_{ges} is the section modulus of total section (mm^3); I_i is the second area moment of considered layer (mm^4); $\beta_{R,i}$ is the compressive strength of considered layer (N/mm^2); γ_i: partial safety factor of considered layer (−)

Based on the stiffness method, calculations for MultiLC-walls and beams (representing elements of the building envelope subjected to bending, such as lintels) were carried out. Experimental tests were performed to determine the load bearing capacity and to show whether any adjustments of the applied calculation methods are needed. Furthermore, a wall-to-slab connection was designed, built and tested to investigate the load transfer from inner normal concrete floor slabs to the inhomogeneous MultiLC elements of the building envelope. The results of these investigations are described in the following chapters.

2 | STRUCTURAL BEHAVIOR OF INHOMOGENEOUS BEAMS

2.1 | Analytical investigation

The main aim of the analytical investigation was to obtain a statement about the maximum load bearing capacity under bending stress and to formulate a design method to determine the area of reinforcement for the multi-layered specimens subjected to bending in the experiments.

Through the relation for the maximum load bearing capacity,[15]

$$M_u = F_c \cdot z \quad (2a)$$

$$M_u = \alpha_R \cdot x \cdot b \cdot f_c^* (d - k_a \cdot x) \quad (2b)$$

where α_R is the solidity coefficient (=0.5)[16]; k_a is the height coefficient (=1/3)[16]; b is the width of cross section; d is the statically effective height; and f_c is the compressive strength.

the height of the concrete compression area x,

$$x = \frac{\varepsilon_c}{\varepsilon_s - \varepsilon_c} \cdot d \quad (3)$$

the equilibrium of inner forces,

$$F_c = F_s \quad (4)$$

and the relation

$$A_s = \frac{F_s}{f_y} \quad (5)$$

both, the maximum load bearing capacity and the area of reinforcement can be determined. Therefore, the strain distribution throughout the cross section is needed (Equation (3)), hence in the concrete layers (ε_C) as well as in the reinforcement (ε_S). Due to an elastic deformation behavior until failure and a stress–strain relation with a triangular shape, solidity coefficient α_R equals 0.5, height coefficient k_a equals 1/3.[16] Still, the cross section of the beam is assumed to remain planar and normal to the deformed axis of the beam, thus the Bernoulli hypothesis is valid. This leads to an equal strain distribution in the concrete layers and also in the reinforcement.
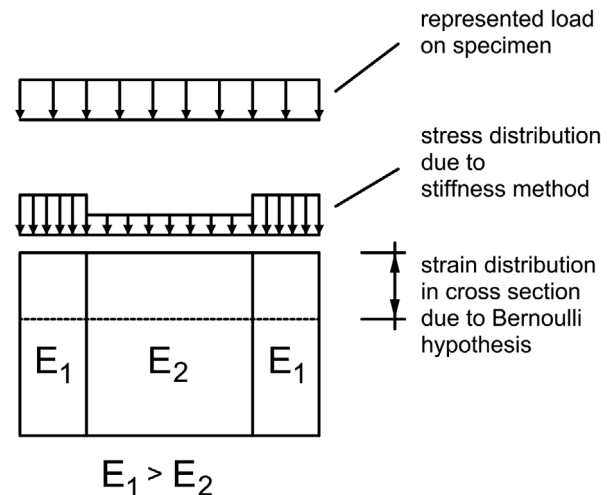

FIGURE 3 Stress/strain distribution in the specimen due to described assumptions

Since the used concretes have different Young's moduli (E), there is an unequal stress distribution caused by equal strain distribution. The "stiffer" concrete attracts more forces compared to the "softer" concrete (Figure 3).

Hence, to guarantee an equal strain distribution and thus a varying stress distribution for a beam under bending stress, the area of reinforcement must be different for each concrete layer.

It is the aim to determine the maximum bending moment and the area of reinforcement which is needed for the load bearing as well as for the heat-insulating concrete. Therefore, Equation (2b) and (5) are needed. The height of the concrete compression area x (Equation (3)) includes the two unknowns of concrete strain ε_C and reinforcement strain ε_S. By limiting the concrete strain to the ultimate compressive strain $\varepsilon_C = \varepsilon_U$ of the softer concrete, there is just the reinforcement strain ε_S as an unknown. It can reach a theoretical value between 0–25 ‰.[15]

By setting a reinforcement strain to a certain value, the maximum bending moment can be determined by Equation (2b), the reinforcement area by Equation (5).

Figure 4 shows the correlation between the reinforcement strain, the maximum bending moment and the reinforcement area for a beam made from an ILC800 and an ILC500. In addition, an example is shown how to determine the maximum bending moment as well as the reinforcement area if the reinforcement strain is set to 7.25 ‰. By following the arrows, it leads to a maximum bending moment of $M_u = 11.41$ kNm. For each shell a reinforcement area of $A_{S,ILC800} = 0.5$ cm² is needed, for the core a reinforcement area of $A_{s,ILC500} = 0.44$ cm² is needed.

2.2 | Experimental investigation

The load bearing behavior of concrete beams with inhomogeneous properties under bending stress was investigated using a total of 14 specimens with different setups in a four point bending test. All specimen had the length of 3.30 m, a width of 0.40 m and a height of 0.20 m. In all cases, the load appears at a distance $a = 1.0$ m of the beam supports (Figure 5). To provide a bending failure,
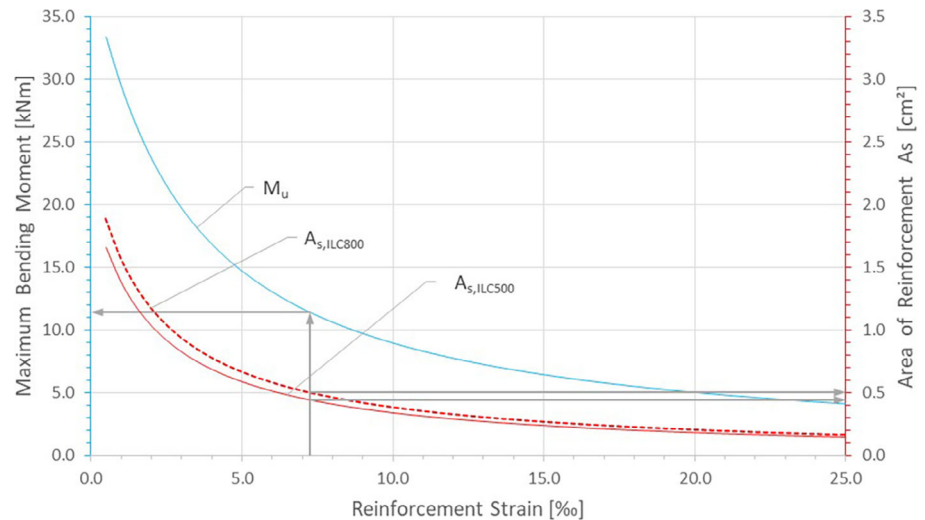

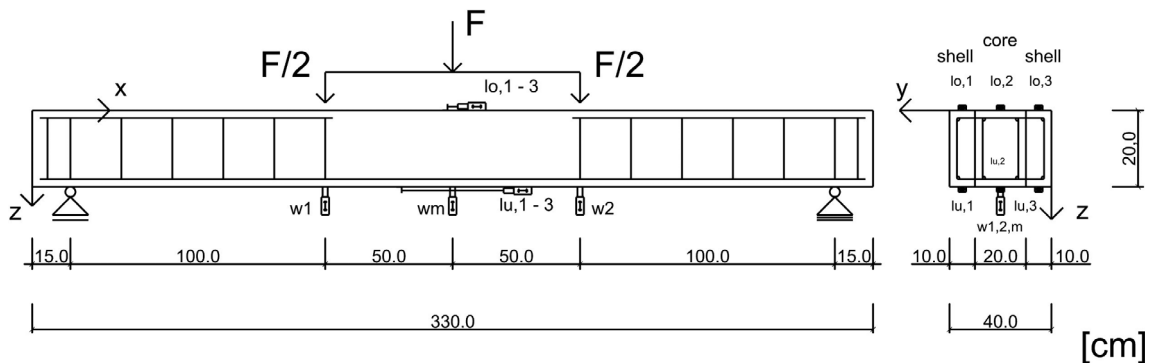**FIGURE 4**   Correlation between M_U, reinforcement strain and A_S

FIGURE 5   Test setup and measurement system for beam specimens in four-point bending test

TABLE 2 Concrete characteristics and test results

Specimen no.	Concrete	Dry density (g/cm^3)	Compressive strength (N/mm^2)	Young's modulus (N/mm^2)
1.1	ILC800	861	13.69	–
	ILC500	464	4.24	1,561
1.2	ILC800	765	13.23	3,531
	ILC500	477	5.32	1,459
1.3	ILC800	741	12.62	5,695
	ILC500	471	3.76	1,366
1.4	ILC800	767	13.95	3,490
	ILC500	497	4.89	1,553

Specimen no.	Maximum bending moment		
	Analytical (kNm)	Experimental (kNm)	$M_{u,ana}/M_{u,exp}$
1.1		14.57	0.78
1.2	11.41	13.64	0.84
1.3		14.52	0.79
1.4		15.31	0.75

the relation between a and the specimen height h should be higher than 3.5.[17] The present dimensions lead to a relation of $a/h = 1.0/0.2 = 5.0 > 3.5$. Otherwise, there will be a high risk of shear failure, which is not the topic of the present investigations. The measurement system ($l_{o,1-3}$, $l_{u,1-3}$ and $w_{1,2,m}$) consisted of extensometers (Figure 5) to determine the deformation behavior, the maximum load bearing moment and also to give a statement about the load distribution between the layers. All specimens were built with a bending reinforcement along the whole length. A shear reinforcement was placed between the load application and the beam support to lower the risk of shear failure.

Since the concrete mixes for the load bearing and insulating concretes were not yet developed at the time of the first beam tests, already existing mixes of ILC as well as a normal concrete with different strength classes and dry densities were used to simulate stiffness differences for the first 10 specimens. Only four specimens were built with the final setup (strong shell; Figure 1) and are discussed in the present paper. The final setup consists of an ILC800 (dry density of less than 800 kg/m^3) as the load-bearing concrete and an ILC500 (dry density of less than 500 kg/m^3) as the heat-insulating concrete. An overview of the characteristics and a comparison of the analytical and experimental maximum bending moment is shown in Table 2.

To investigate the load distribution across the cross section, two specimens were tested with a full load application over the whole cross section (no. 1.1/1.2), another two with a partial load application only in the load-bearing layers (no. 1.3/1.4) using steel plates for the load application (cf. Figure 6).
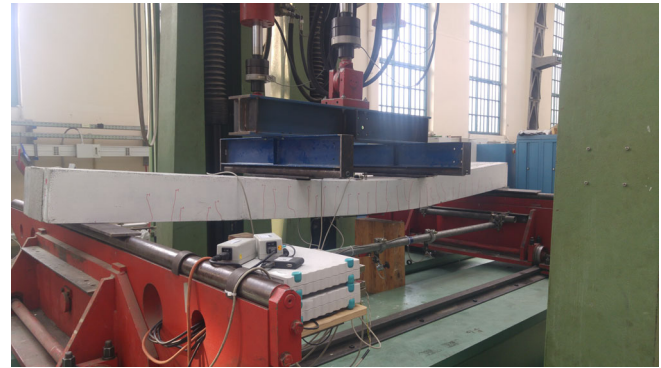
FIGURE 6 Specimen in a four-point bending test

2.3 | Discussion

The aim was to develop design requirements for multi-layered beams under bending stress. Especially the maximum load bearing capacity was of interest. The correct hypotheses were to be identified through a comparison of the analytical and experimental investigation, as well as the limitations of the set design concept. The following section focuses on the final setup.

Based on the analytical and experimental results, it was possible to formulate a first approach to determine the maximum bending moment M_u for inhomogeneous beams based on the stiffness method. Also, a design approach to derive M_{Rd} can be recommended using design values in the calculation method of M_U described above. This design approach needs to fulfill the boundaries of the three fundamental assumptions for designing

a concrete beam: the equilibrium condition of external and internal forces, the validity of the Bernoulli hypothesis, hence equal strains in the concrete layers and the material laws. The latter includes the maximum strain for the concrete. The maximum strains of ILC-concretes differ from each other. With respect to the Bernoulli hypothesis, the concrete with the lower maximum strain governs the limit for the maximum strain of the cross-section.

Compared to the experimental investigations, the calculation of the maximum bending moment M_u based on the mean compressive cylinder strength leads to a conservative result. However, due to the standard range of different bar diameters available, it was not possible to place exactly the required area of reinforcement. The actual area of reinforcement is always higher compared to the analytical; hence it influences the strain distribution.

The experimental tests also showed that an interaction between the insulating and the load-bearing layer regarding the load transfer could be identified. Furthermore, no significant difference regarding the maximum bending moment between a partial and a full load application was observed. However, partial load application resulted in shear cracks between the layers.

3 | STRUCTURAL BEHAVIOR OF INHOMOGENEOUS WALLS

3.1 | Analytical determination of load bearing capacity and design approach

As discussed in Chapter 1, the stiffness method was chosen to determine the load bearing capacity of inhomogeneous MultiLC-walls. For centric, vertical loading (no bending), the ultimate axial load $N_{u,cal}$ of the whole cross-section was derived based on Equation (1), using the following expressions:

$$N_{u,cal} = \sum_{i=1}^{n} \sigma_i \cdot A_i$$

$$\text{and } \sigma_i = \left(\frac{N_{u,cal}}{A_i} \cdot \frac{E_i \cdot A_i}{\sum_{i=1}^{n} E_i \cdot A_i} \right) \leq f_{cm,cyl,i} \left[\text{N/mm}^2 \right] \quad (6)$$

where i is the considered layer; n is the total number of layers; σ_i is the stress of considered layer (N/mm²); $N_{u,cal}$ is the ultimate vertical load (N); E_i is the Young's modulus of considered layer (N/mm²); A_i is the area of considered layer (mm²); $f_{cm,cyl,i}$ is the mean compressive cylinder strength of considered layer (N/mm²)

The limiting criteria of $\sigma_i \leq f_{cm,cyl,i}$ lead to the definition of $N_{u,cal}$. The proportional distribution of the load between layers is defined by the term $\frac{E_i \cdot A_i}{\sum_{i=1}^{n} E_i \cdot A_i}$.

For the design values of axial resistance N_{Rd}, it is proposed to use the approach for plain concrete walls defined in Eurocode 2 (EC2 section 12),[18] assuming homogeneous support at the wall base and homogeneous, centric loading at the wall top:

$$N_{Rd,\lambda} = b \cdot h_w \cdot f_{cd,pl} \cdot \phi \quad (7)$$

where $N_{Rd,\lambda}$ is the axial resistance (N); b/h_w is the width/thickness of cross section (mm); $f_{cd,pl}$ is the design compressive strength of plain concrete (N/mm²); Φ is the factor taking eccentricity into account

As a conservative measure, it is suggested to only consider the load-bearing capacity of the load-bearing shell layers. This would account for the possibilities of partial loading only in the load-bearing shell layers and/or a very porous core concrete with very low strength. Reinforcement will be designed only according to minimum and crack control requirements of EC2.[18] It is proposed to neglect reinforcement for design in ultimate limit state.

3.2 | Experimental examination

To verify the analytical approach described above via experimental examination, preliminary tests on small-scale inhomogeneous specimens (cubes 15/15/15 (cm³) and prisms 15/15/22.5 (cm³)) were carried out as a first step. In test series 1, the load was applied over the whole cross section, hence evenly over the two different layers (Figure 7a). In test series 2, the load was applied partially only in the load bearing layers, hence the shell layers as shown in Figure 1. The partial loading was conducted via steel plates between the testing equipment and the load bearing layer (Figure 7b).

For Series 1, the maximum load determined via the stiffness method gave conservative results compared with the experimental results. For Series 2, the experimental maximum load was in the range of the compressive strength of the load-bearing layer, which was to be expected due to partial loading and limited specimen height, hence limited load distribution to the insulating (core) layer. For both series, failure occurred predominantly in the load-bearing layers. Figure 7c,d exemplarily show the wedge-shaped crack pattern underneath the load application, followed by vertical cracking, of a partially loaded specimen of Series 2.

In the second step, experimental tests on six wall specimens, produced at TU Berlin, were carried out. The dimensions were chosen according to the criteria for
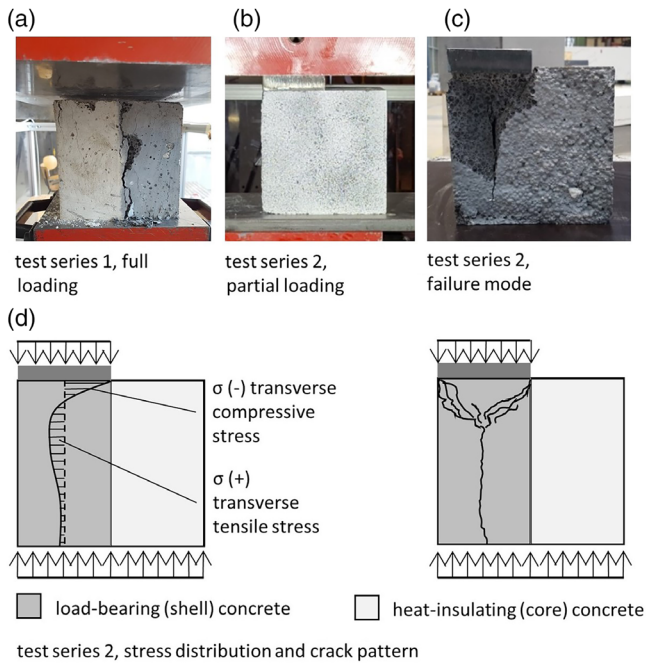
FIGURE 7 Test setup and failure mode of load capacity tests with inhomogeneous cubes (based on[19])

walls ($b/h > 4$) and to represent a story height of 3 m at the scale of 1:2, resulting in a specimen height of 1.5 m and a cross section of 0.225mx1m. All walls had a different setup (Figure 8, left). Specimen 1.1–1.3 represented a three-layer setup, walls 1.5 and 1.6 a two-layer setup (layers consisted of ILC800 and ILC600, mixes according to[1]). Specimen 1.4 also represents a three-layer setup, but without core concrete, thus simulating a case where the inner core layer has extremely low density and hence next to no strength. The reinforcement of the walls was chosen according to crack width control requirements as described in EC2,[18] in this case vertical and horizontal bars $d = 8$ mm, spacing 12 cm. Walls 1.1 and 1.6 had additional stirrups in top and bottom. Stirrups along the vertical planes were neglected to not prevent any delamination of layers that might occur due to loading of walls with realistic horizontal length. To further increase the bond between the ILC layers, horizontal bars of glass fiber reinforcement were added.
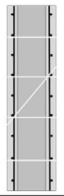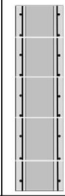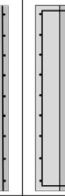
The specimens were loaded either over the whole cross-section or partially only in the load-bearing shell layers (Figure 8). The measuring equipment consisted mainly of strain gauges in the top and bottom area of the front faces of the walls. Besides determination of the maximum load-bearing capacity, the goal was to investigate the load distribution in the load application area between load-bearing shell and insulating core layers and the load reactions in the layers at the base point. Figure 8 (right) shows a comparison of the calculated maximum loads $N_{u,cal}$ and the results of the experimental tests $N_{u,exp}$.

As shown in Figure 8 (right), in all tests, the expected maximum load $N_{u,cal}$ calculated via the stiffness method, taking the mean cylindrical compressive strength into account, was not reached. Full loading over the whole cross section resulted in higher experimental maximum loads $N_{u,exp}$ (approx. 60% of expected load $N_{u,cal}$; specimen 1.2 and 1.5) than partial loading (between approx. 30–40% of expected load $N_{u,cal}$). Failure occurred mainly due to vertical cracking in the load-bearing layers, often coinciding with the longitudinal reinforcement layer, with a similar pattern to the failure of the preliminary small scale tests. The strain measurements at the base point confirmed the predicted load distribution between layers according to the stiffness method not quantitatively, but qualitatively.

One of the main reasons for not reaching the predicted loads was seen in the setup of load application and testing machinery, where several issues pointed to a need for improvement. The second cause was suspected in the assumption of the mean cylinder compressive strength for calculating the load bearing capacity $N_{u,cal}$. These two aspects were further investigated. The methodology and results are described in more detail in the final project report.[20] Consequently, the test setup and machinery were altered by several measures. Special emphasis was placed on ensuring centric loading using, for example, different types of coatings between top and bottom of the specimen and the test equipment.

Regarding the expected strength of the wall specimen under testing conditions, several influencing factors were investigated. It was found that already for a testing time span of about 30 min, long-term effects must be taken into account. Experimental examinations during and after the MultiLC-project[20,21] were carried out in several test series on ILC-cylinder specimens (32 in total). The specimens were subjected to continuous loading at levels of 70–85% of the short-term mean compressive cylinder strength $f_{cm,cyl}$. The load was kept constant until the specimen failed or, if no failure occurred after 1 hr, the load was increased until failure. The results suggested that even for a comparatively short time span of 20–30 min failure occurs at a level of approx. 85% of the short-term strength, hence indicating a value for long-term effects of $\alpha_{cc,30\ min} = 0.85$. Since this type of test is very sensitive to variances in material strength (the short-term strength has to be derived from other cylinders than the ones subjected to long-term loading), more tests are recommended for statistical validation.

In addition to long-term effects, it also should be considered that the strength of a laboratory cylinder specimen is expected to be 15% higher than the strength of an in-situ structure or structural component ($\gamma_{conv} = 1.15$).[22] Hence, according to the code[23] a structural element meets the requirements if its strength is approx. 85% of the cylinder
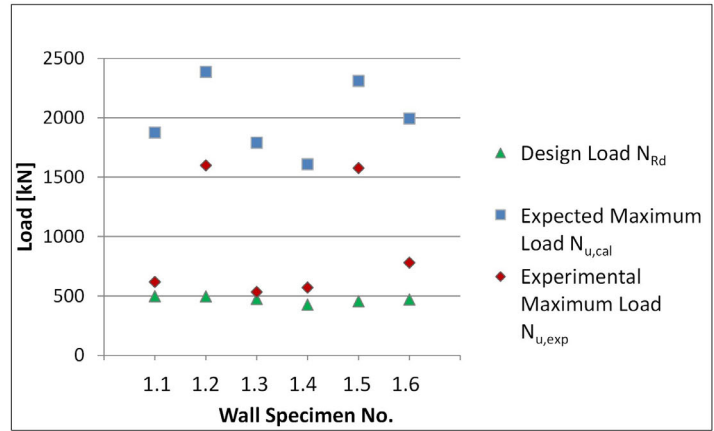
FIGURE 8 left: test program with inhomogeneous walls (based on[19]); right: comparison of experimental results, predicted maximum loads and design loads

strength. Further aspects such as size effect and slenderness need to be considered and are currently being investigated. First results suggest a significant influence of the higher wall slenderness compared to a cylinder specimen. However, these effects are neglected for now on the conservative side in the context of this paper.

Thus, the required strength of the layers of the inhomogeneous wall elements under experimental testing conditions $f_{e,i}$ is suggested to

$$f_{e,i} = \alpha_{cc,30\,min} \cdot \frac{f_{cm,cyl,i}}{\gamma_{conv}} = 0.85 \cdot \frac{f_{cm,cyl,i}}{1.15} = 0.74 \cdot f_{cm,cyl,i} \quad (8)$$

The required experimental strength $f_{e,i}$ should be interpreted as the minimum strength the structural element has to possess in order to meet the requirements of the code.

After reconditioning of the testing machinery and alteration of the test setup, two more wall specimens were examined (setup see Figure 9, mixes ILC800 and 500 see Table 1). The thickness of the load-bearing shell layer was set to 10 cm to reflect 1:1 scale conditions in combination with the reinforcement. The thickness of the core layer was set to 12.5 cm. Both walls were subjected to full, centric vertical loading. The expected maximum load $N_{u,cal}$ was determined via the stiffness method using the required experimental strength $f_{e,i}$ instead of the mean compressive cylinder strength $f_{cm,cyl,i}$.

As shown in Figure 9 (right), the experimental maximum load $N_{u,exp}$ was approx. 90% and 115% of the expected maximum load $N_{u,cal}$, based on $f_{e,i}$. Both specimens showed a failure mode and crack patterns similar to the previous tests.
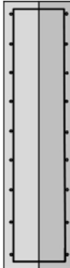
3.3 | Discussion

From the analytical and experimental investigation outlined above one can conclude that the stiffness method is a reasonable approach to predict maximum load-bearing capacity of inhomogeneous MultiLC-walls subjected to centric, vertical loading. However, the required strength of the wall specimen $f_{e,i}$ under testing conditions is not equal to the mean cylinder compressive strength $f_{cm,cyl,i}$ but significantly lower. The last two tests indicate that the stiffness method in combination with the proposed $f_{e,i}$ can reflect the real resistance of the elements more precisely. More tests are needed to verify this approach statistically. Furthermore, other aspects influencing $f_{e,i}$ have to be considered, such as size effect and slenderness.

As described, $f_{e,i}$ should be interpreted as the strength that is required of the structural element to be consistent with the code. This means that the proposed approach for determination of the design values of axial resistance N_{Rd} of the inhomogeneous elements can still considered to be valid.

4 | STRUCTURAL BEHAVIOR OF WALL-TO-SLAB CONNECTION

For a holistic investigation of a building envelope a wall-to-slab connection, hence the connection of a multi layered ILC-wall and a normal concrete floor slab was also of interest. The slab connection can be carried out either hinged or fixed. Hinged connections come with the advantage of lower stress introduction into the walls and seem therefore preferable for materials with lower

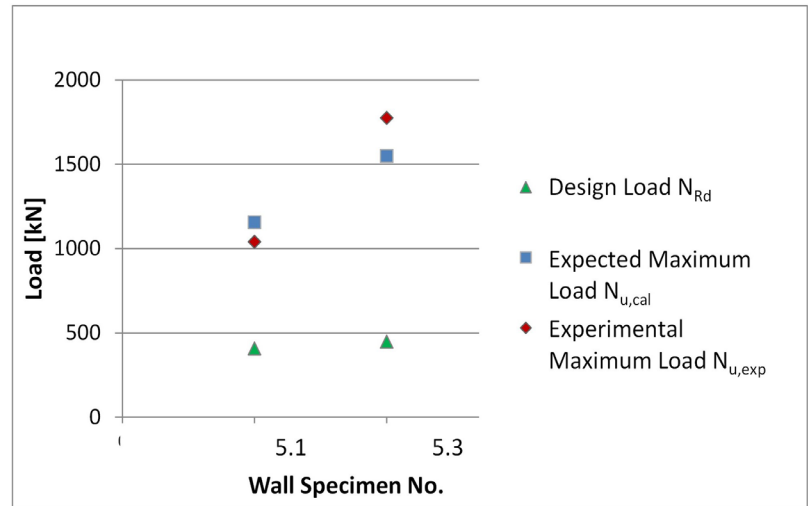| wall specimen no.	5.1	5.3
ILC types: (dry densities in [kg/m³])	800-500	
layer depths [cm]:	10-12.5	
full loading		

FIGURE 9   left: setup of wall specimen; right: comparison of experimental results, predicted maximum loads and design loads

strengths such as ILC. However, fixed connections allow for longer slab spans due to lower field moments. Furthermore, the considerable wall thickness of ILC-walls already imply a certain degree of clamping, even with a hinged connection. Therefore, the feasibility of a fixed slab connection to a multi-layered ILC wall was investigated. The structural detail was developed, built and tested in a first trial of a prototype.

An eight story reference building (Figure 10)[24] was used as a sample for loading and geometry and a representative combination of vertical load and clamping moment in one of the connecting points was chosen. In the first step, the connection was analytically and numerically examined,[20,25,26] focussing on the load transfer from the comparatively stiff normal concrete floor slab to the rather soft shell and core layers of the MultiLC-wall. With respect to the previous chapters, compression and tension resulting from the clamping moment were expected to be transferred predominantly to the stiffer shell layers of the wall.

As a result of the analytical investigations, a strut and tie model is shown in Figure 11. It demonstrates the expected loads during service load state in the floor slab as well as in the constituent wall layers. Additionally, numerical investigations implemented as a FE-Analysis by SOFISTIK (Figure 12)[25] were carried out. Based on the analytical and numerical investigations, the wall segment underneath the slab was expected to experience full compression when subjected to dead load and service load at design level (vertical load of 280.0 kN from the wall segment above and vertical load of 21.0 kN on the floor slab). The loading was chosen to create a representative combination of vertical load and clamping moment from the reference building as mentioned above and does

not represent ultimate or serviceability limit state. The structural detailing, hence the needed reinforcement was determined for the specimens due to these results.

The experimental investigation contained two specimens shown in Figure 11. As a measuring system, an optical deformation analysis provided by an ARAMIS System was chosen. It records the relative deformation in a marked area shown in Figure 15. Within the experiments, it was shown that the load bearing capacity exceeded the expected service load. Figure 13 shows the present deformation in x- and y-direction at service load of specimen 1 (blue: compression, red: tension). The wall underneath the slab connection is under full compression. However, there is a higher deformation at the slab facing side of the wall. This behavior coincides with the forces shown in the strut and tie model as well as the principal stresses of the FE-analyses.

After analyzing the deformation at service design load (21.0 kN on the floor slab), the load introduced to the floor slab was raised to a maximum of 98.87 kN and stopped at that level due to the setup of the testing equipment. The specimen showed no sign of failure at this point. The deformation under that load is shown in Figure 14. Due to the high load on the slab, tension resulting from the clamping moment outweighs compression from the vertical loading in the outer layer of the wall. Hence, the wall experiences tension as well as compression. Also, the deformation analysis shows that the main deformation, hence the main forces of both, compression and tension, are present in the outer shell layers of the wall.

As a conclusion, the investigations show the feasibility of a fixed connection between a normal concrete slab and a multi-layered ILC-wall. The transfer of the clamping moment from the slab to the shell and core layers of the

wall is possible. As expected according to the stiffness method and due to the stress distribution of the clamping moment, the shell layers experience a load concentration

compared to the core layer. There were no flaking at the wall-slab connection or critical cracks regarding the serviceability detected. As a next step, further investigations should be carried out to derive a design approach.

FIGURE 10   Reference Building[24]

5 | CONCLUSION

Multi-functional lightweight concrete elements with inhomogeneous properties are a contribution to high-performance materials for the building skin. By an increase in efficiency of building elements a reduction of energy and resources consumption can be achieved, and sustainability thus be enhanced. For the development of such highly efficient MultiLC-elements, investigations in concrete technology and building physics as well as investigations about the structural behavior of wall and beam specimens and wall-to-slab connections are of high importance. Infra-Lightweight Concretes with dry densities between 500 and 800 kg/m^3 were combined to create areas with different properties according to load bearing and insulation functions within the cross-section, thus increasing performance. In order to describe the structural behavior of such inhomogeneous elements, the stiffness method was chosen from various approaches. Based on this method, analytical, experimental and numerical investigations were
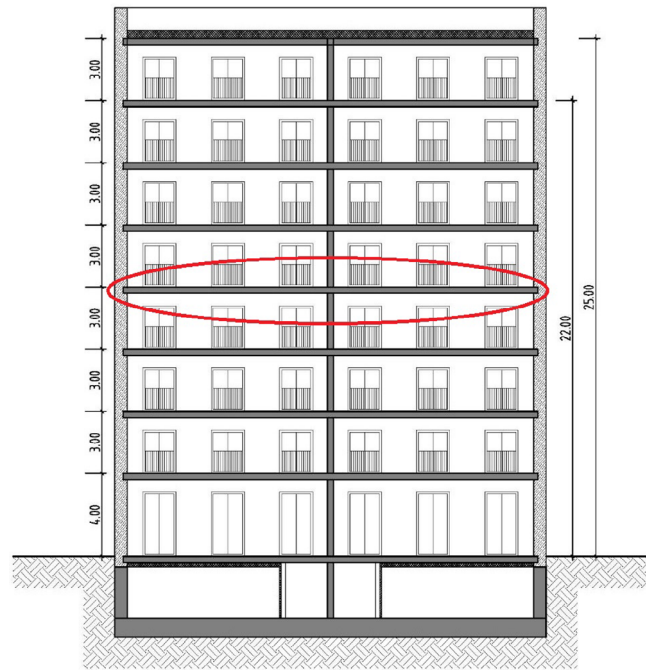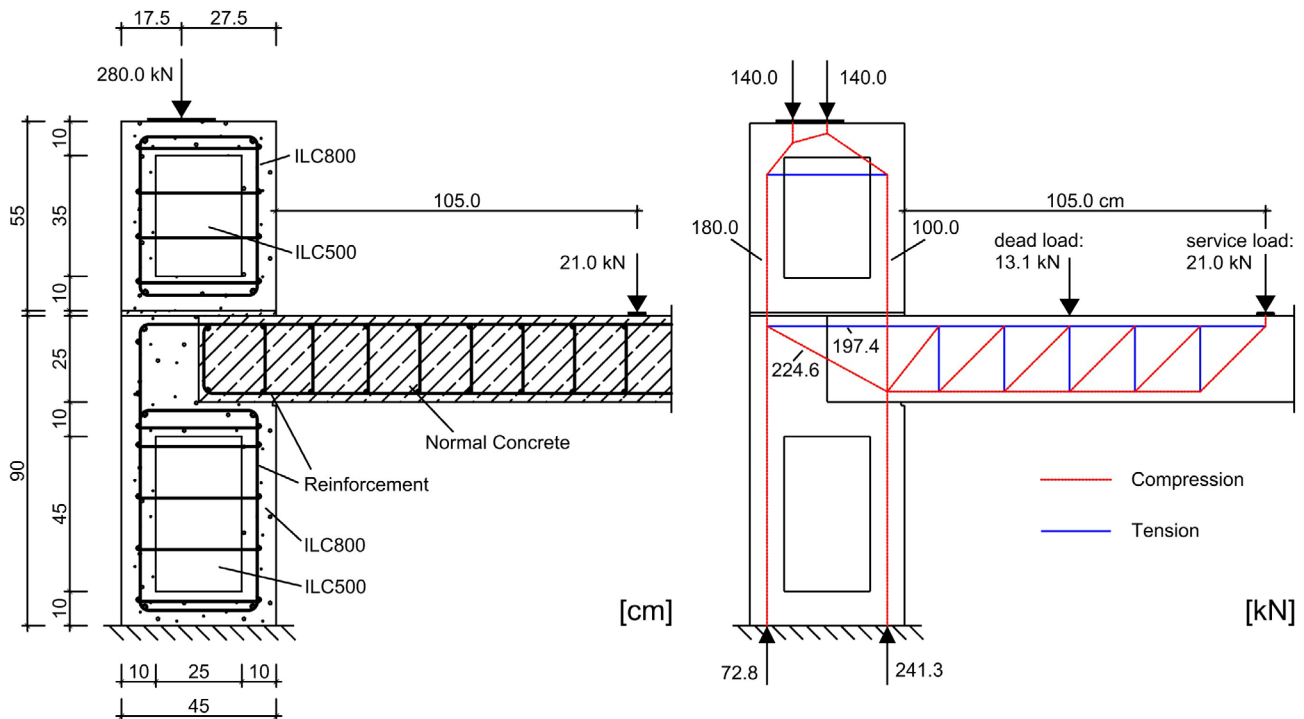

FIGURE 11   left: geometry and reinforcement of the specimen; right: strut and tie model under service load
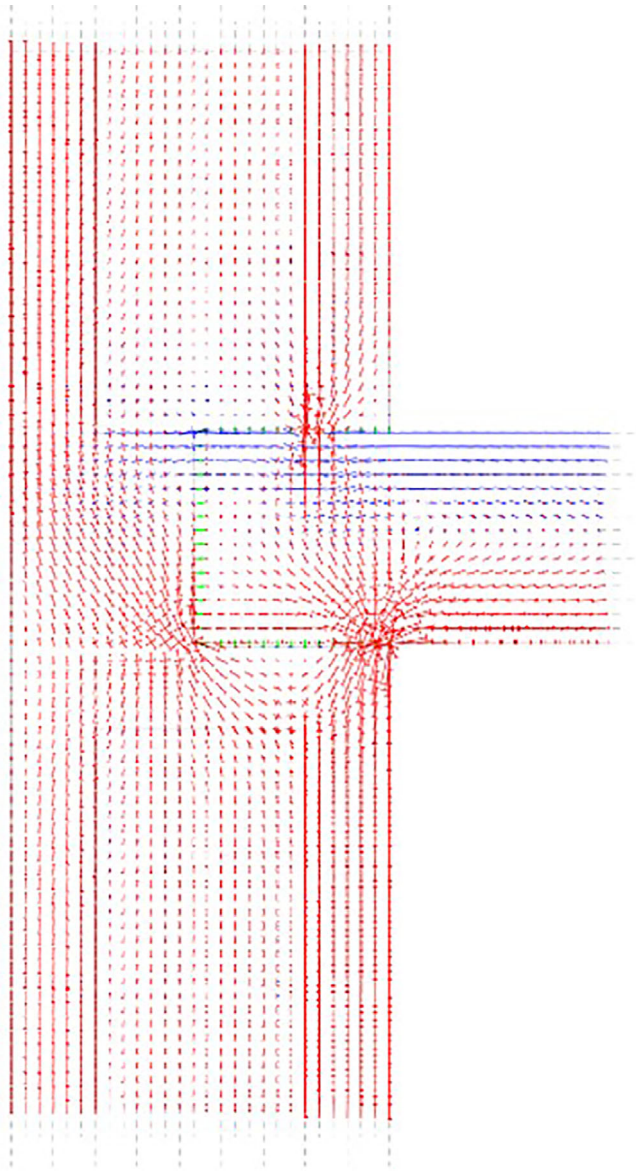
FIGURE 12   Principle stress; blue: tension; red: compression[25]

carried out to describe the load bearing behavior of inhomogeneous beams, walls and wall-to-slab connections. It was possible to formulate a first approach to determine the maximum bending moment M_u for inhomogeneous beams based on the stiffness method. From the analytical and experimental investigation outlined above one can conclude that the stiffness method is a reasonable approach to predict maximum load-bearing capacity of inhomogeneous MultiLC-walls subjected to centric, vertical loading. It was also found that the required strength of a wall specimen $f_{e,i}$ under testing conditions is not equal to the mean cylinder compressive strength $f_{cm,cyl,i}$ but significantly lower. First recommendations could be formulated for the design of inhomogeneous MultiLC-walls and

MultiLC-beams. Furthermore, the feasibility of a fixed connection between a normal concrete slab and a multi-layered ILC-wall was shown. In a next step, the proposed calculation and design approaches should be verified by further investigations.

DATA AVAILABILITY STATEMENT
N/A

NOTATION

|	
A_{ges}	total area of section, mm^2
A_i	area of considered layer, mm^2
A_s	area of reinforcement, mm^2
b	width of cross section, mm
d	statically effective height, mm
E_i	Young's modulus of considered layer, N/mm^2
F_c	internal compression force, N
f_c	compressive strength, N/mm^2
$f_{cd,pl}$	design compressive strength of plain concrete, N/mm^2
$f_{cm,cyl,i}$	mean compressive cylinder strength of considered layer, N/mm^2
$f_{e,i}$	required strength of considered layer under experimental testing conditions, N/mm^2
F_s	internal tension force, N
f_y	yield strength of reinforcement, N/mm^2
h_w	thickness of cross section, mm
i	considered layer
I_i	second area moment of considered layer, mm^4
k_a	height coefficient
M	bending moment, Nmm
M_u	ultimate bending moment, Nmm
n	total number of layers
N	axial load, N
$N_{Rd,\lambda}$	axial resistance, N
$N_{u,cal}$	ultimate vertical load, N
W_{ges}	section modulus of total section, mm^3
x	height of the concrete compression area, mm
z	internal lever arm, mm
$\alpha_{cc,30}$ min	coefficient taking account of long term effects on the compressive strength over a period of 30 min
α_R	solidity coefficient
$\beta_{R,i}$	compressive strength of considered layer, N/mm^2

ε_c c
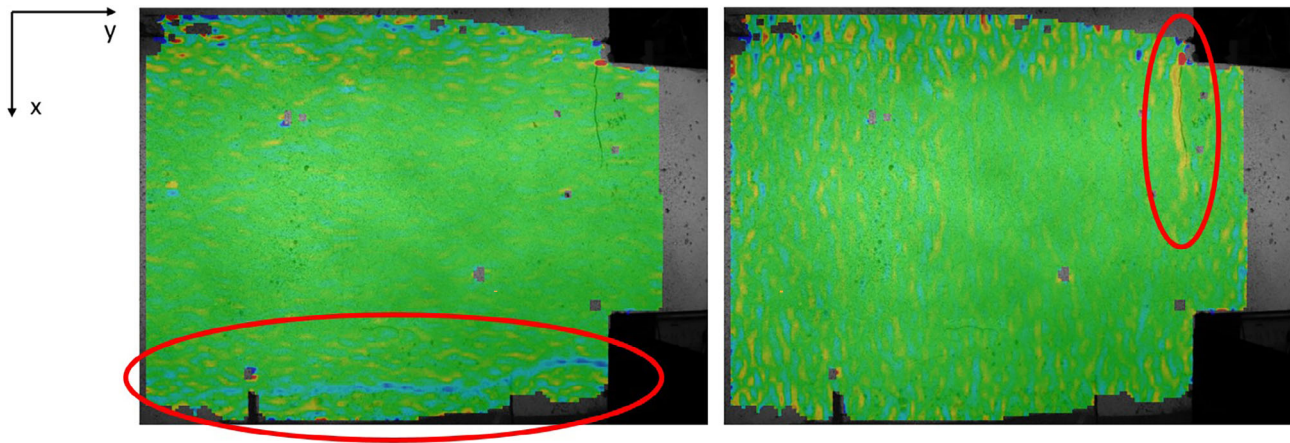
FIGURE 13 Deformation under service load; left: *x*-direction; right: *y*-direction
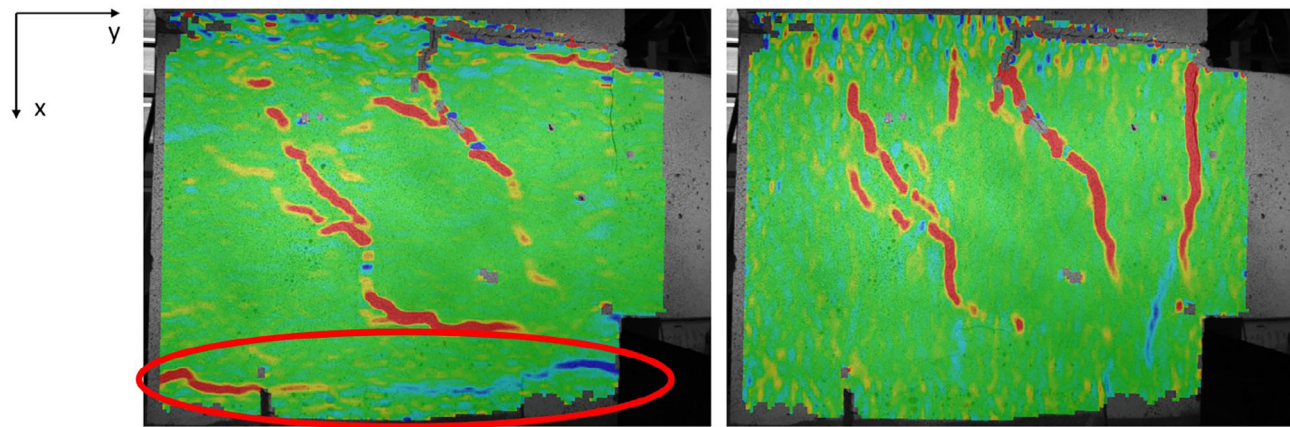

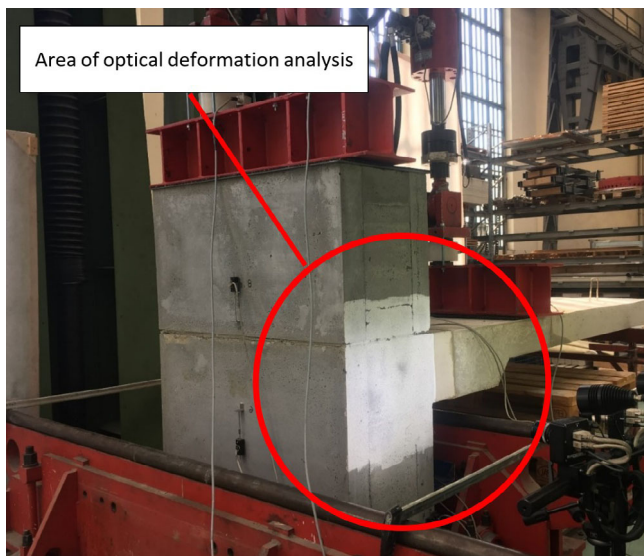**FIGURE 14** Deformation at maximum load; left: *x*-direction; right: *y*-direction

FIGURE 15 Specimen and area of optical deformation analysis

ε_s	reinforcement strain
σ_i	stress of considered layer, N/mm^2
Φ	factor taking eccentricity into account

ORCID

Claudia Lösch https://orcid.org/0000-0003-1957-1834

REFERENCES

1. Hückler A, Schlaich M. Structural behavior of reinforced infra-lightweight concrete (ILC). ACI Struct J. 2019;116:3–14.
2. Schlaich M, Hückler A. Infraleichtbeton: Reif für die Praxis. Beton Stahlbetonbau. 2017;112(12):772–783.
3. Schlaich M, Hückler A, Lösch C. Infra-lightweight concrete—A monolithic building skin. In: Auer T, Knaack U, Schneider J, editors. Proceedings of the Powerskin Conference January 19th 2017, Munich. Delft, the Netherlands: TU Delft, 2017; p. 293–303.
4. Kieback B, Neubrand A, Riedel H. Processing techniques for functionally graded materials. Mater Sci Eng. 2003;A 362:81–106.

5. Heinz P. Gradientenwerkstoffe und Architektur (Diplomarbeit). Stuttgart: Universität Stuttgart, Institut für Leichtbau, Entwerfen und Konstruieren (ILEK), 2007.

6. Herrmann M, Sobek W. Functionally graded concrete: Numerical design methods and experimental tests of mass-optimized structural components. Struct Concr. 2017;18(1):54–66.

7. Fontana P, Miccoli L, Kocadag R, et al. Composite UHPC facade elements with functional surfaces. In: Fehling E, editor. Ultra-High Performance Concrete and High Performance Construction Materials: Proceedings of HiPerMat. Volume 2016. Kassel, Germany: Kassel University Press GmbH, 2016.

8. Lösch C, Stephan D, Schlaich M, Vogdt FU. Multifunktionale Leichtbetonbauteile mit inhomogenen Eigenschaften (MultiLC). HighTechMatBau—Neue Materialien im Bauwesen: Tagungsband mit Beiträgen zur Konferenz vom 31. Januar 2018 in Berlin. Stuttgart: Fraunhofer IRB, 2018; p. 49–53.

9. Neumann M. Entwicklung von Verfahren zur Beurteilung des Tragverhaltens von mehrschichtigen Außenwandelementen aus Betonen unterschiedlicher baustofflicher Kennwerte (Dissertation). Weimar: Bauhaus-Universität Weimar, Fakultät Bauingenieurwesen, 1997.

10. Trätner A. Sanierungsgrundlagen Plattenbau: Tragverhalten von Außenwandlementen aus haufwerksporigem Leichtbeton nach TGL. Stuttgart: Fraunhofer IRB Verlag, 2000.

11. Herrmann M, Haase W. Tragverhalten biege- und querkraftbeanspruchter Bauteile aus funktional gradiertem Beton. BUST. 2013;108(6):382–394.

12. Pietras D, Sadowski T. A numerical model for description of mechanical behaviour of a functionally graded autoclaved aerated concrete created on the basis of experimental results for homogenous autoclaved aerated concretes with different porosities. Construct Build Mater. 2019;204:839–848.

13. Lösch C, Richter A, Schlaich M. Multifunctional inhomogeneous lightweight concrete elements—Outline and structural behaviour. Tomorrow's megastructures: 40th IABSE Symposium 2018: Nantes, France, 19–21 September 2018. Red Hook, NY: Curran Associates Inc, 2018; p. 3.

14. Wagner E, Vargas E, Dietermann M, et al. Multifunktionale Leichtbetonbauteile mit inhomogenen Eigenschaften - Ergebnisse der Arbeitsgruppe Betontechnologie aus dem Verbundprojekt MultiLC. Deutscher Beton Bautechnik-Verein DBV Rundschreiben. 2019;263:7–10.

15. Zilch K, Zehetmaier G. Bemessung im konstruktiven Betonbau: Nach DIN 1045–1 (Fassung 2008) und EN 1992-1-1 (Eurocode 2). Berlin: Springer eBooks, 2010.

16. Hückler A, Schlaich M. Zur Biegung von Infraleichtbetonbauteilen—Werkstoff-, Verbund-, Trag- und Verformungsverhalten. Beton- Stahlbetonbau. 2017;112(5):282–292.

17. Leonhardt F, Mönnig E. Vorlesungen über Massivbau—Teil 1: Grundlagen zur Bemessung im Stahlbetonbau. Berlin, Heidelberg: Springer, 1984.

18. DIN Deutsches Institut für Normung e.V. 2011. Eurocode 2: Bemessung und Konstruktion von Stahlbeton- und Spannbetontragwerken—Teil 1–1: Allgemeine Bemessungsregeln und Regeln für den Hochbau; Deutsche Fassung EN 1992-1-1:2004 + AC:2010, Beuth Verlag, ICS 91.010.30; 91.080.40, DIN EN 1992-1-1/NA.

19. Hahnemann D. Multifunktionale Leichtbetonbauteile - Untersuchung von Wandscheiben aus inhomogenem Leichtbeton. Berlin: Technische Universität Berlin, 2017.

20. Stephan D, Schlaich M, Vogdt FU, et al. Multifunktionale Leichtbetonbauteile mit inhomogenen Eigenschaften (MultiLC)—Mechanische, Bauchemische und Bauphysikalische Untersuchungen: Abschlussbericht zum Forschungsprojekt. Berlin: Bundesministerium für Bildung und Forschung, 2019.

21. Jünke D. Bauteilfestigkeit von ILC-Wänden (Masterarbeit). Berlin: Technische Universität Berlin, Bauingenieurwesen, 2019.

22. Fingerloos F, Hegger J, Zilch K. Eurocode 2 für Deutschland: DIN EN 1-1-1992 Bemessung und Konstruktion von Stahlbeton- und Spannbetontragwerken; Teil 1–1: Allgemeine Bemessungsregeln und Regeln für den Hochbau mit Nationalem: Anhang Kommentierte Fassung. 2. Überarbeitete Auflage 2016, Beuth. Berlin: Ernst & Sohn, 2016.

23. DIN Deutsches Institut für Normung e.V. 2008. Bewertung der Druckfestigkeit von Beton in Bauwerken oder in Bauwerksteilen; Deutsche Fassung EN 13791:2007, Beuth Verlag, V. 91.080.40, DIN EN 13791.

24. Leibinger R, Schlaich M, Lösch C, Rieseberg P, Ballestrem M. Infraleichtbeton im Geschosswohnungsbau (INBIG): Abschlussbericht zum Forschungsprojekt. Zukunft Bau: Bundesinstitut für Baustadt- und Raumforschung im Bundesamt für Bauwesen und Raumordnung, Fraunhofer IRB Verlag, 2017.

25. Kummetat N. Multifunktionale Leichtbetonbauteile—Numerische Bemessung inhomogener Bauteile mit Sofistik (Masterarbeit). Berlin: Technische Universität Berlin, 2017.

26. Reyher B. Multifunktionale Leichtbetonbauteile mit inhomogenen Eigenschaften (MultiLC), Ausführlicher Sachbericht (Schlussbericht). Bundesministerium für Bildung und Forschung. 2019.

AUTHOR BIOGRAPHIES

CLAUDIA LÖSCH, Research Assistant, Chair of Conceptual and Structural Design, Technische Universität Berlin, Berlin, Germany. Email: claudia.loesch@tu-berlin.de.

ARNO RICHTER, Research Assistant, Chair of Conceptual and Structural Design, Technische Universität Berlin, Berlin, Germany. Email: arno.richter@tu-berlin.de.

MIKE SCHLAICH, Professor, Chair of Conceptual and Structural Design, Technische Universität Berlin, Berlin, Germany. Email: mike.schlaich@tu-berlin.de.